# Spin dynamics of quadrupole nuclei in InGaAs quantum dots

M. S. Kuznetsova,[1] R. V. Cherbunin,[1] I. Ya. Gerlovin,[2] I. V. Ignatiev,[1,2] S. Yu. Verbin,[1]
D. R. Yakovlev,[3,4] D. Reuter,[5] A. D. Wieck,[6] and M. Bayer[3,4]
[1]*Saint Petersburg State University, 198504 St. Petersburg, Russia*
[2]*Spin Optics Laboratory, Saint Petersburg State University, 198504 St. Petersburg, Russia*
[3]*Experimentelle Physik 2, Technische Universität Dortmund, D-44221 Dortmund, Germany*
[4]*Ioffe Physical-Technical Institute, Russian Academy of Sciences, 194021 St. Petersburg, Russia*
[5]*Department Physik, Universität Paderborn, 33098 Paderborn, Germany*
[6]*Angewandte Festkörperphysik, Ruhr-Universität Bochum, D-44780 Bochum, Germany*
(Received 29 September 2016; revised manuscript received 27 January 2017; published 19 April 2017)

Photoluminescence polarization is experimentally studied for samples with (In,Ga)As/GaAs self-assembled quantum dots in transverse magnetic field (Hanle effect) under slow modulation of the excitation light polarization from fractions of Hz to tens of kHz. The polarization reflects the evolution of strongly coupled electron-nuclear spin systems in the quantum dots. Strong modification of the Hanle curves under variation of the modulation period is attributed to the peculiarities of the spin dynamics of quadrupole nuclei, which states are split due to deformation of the crystal lattice in the quantum dots. Analysis of the Hanle curves is fulfilled in the framework of a phenomenological model considering a separate dynamics of a nuclear field $B_{Nd}$ determined by polarization of the $\pm 1/2$ nuclear spin states and of a nuclear field $B_{Nq}$ determined by polarization of the split-off states $\pm 3/2$, $\pm 5/2$, etc. It is found that the characteristic relaxation time for the nuclear field $B_{Nd}$ is of order a fraction of a second, while the relaxation of the field $B_{Nq}$ is faster by about two orders of magnitude.

DOI: 10.1103/PhysRevB.95.155312

## I. INTRODUCTION

Hyperfine interaction of an electron localized in a quantum dot (QD) with nuclear spins forms a strongly coupled electron-nuclear spin system [1,2]. This system is considered to be promising for realization of quantum information processing devices [3–5]. The realization of spin qubits assumes some stability of the spin system required for the storage and processing of quantum information. In QDs, the optically polarized electron transfers its spin moment into the nuclear subsystem where the spin orientation may be conserved for a long time controlled by nuclear spin relaxation processes.

The main process destroying the nuclear spin polarization is believed to be the transverse relaxation in local fields caused by the dipole-dipole interaction of neighboring nuclear spins. Characteristic time of the relaxation, $T_2$, for nuclei with spins $I = 1/2$ is of order $10^{-4}$ s [1]. The effective local fields, $B_{dd}$, are a fraction of a millitesla and can be easily suppressed by external magnetic fields exceeding these local fields.

In the case of self-assembled QDs, the stabilization of nuclear spin orientation is possible, in principle, in the absence of external magnetic field [6]. Due to noticeable difference in the lattice constants of QDs and barrier layers, some elastic stress appears in the QDs causing mechanical deformation of the crystal lattice. The deformation results in a gradient of crystal fields acting on nuclei from neighboring atoms and splitting the nuclear spin states for quadrupole nuclei with $I > 1/2$ [1]. Because the strain-induced quadrupole splitting in self-assembled QDs typically greatly exceeds Zeeman splitting in the local fields, the spin orientation of quadrupole nuclei is pinned to the principal deformation axis and is not destroyed by the dipole-dipole interaction [7]. In this case, the stability of the nuclear spin system should be determined by processes of longitudinal spin relaxation of quadrupole nuclei with characteristic time $T_1 \gg T_2$. Although many publications are devoted to the nuclear spin polarization [6,8–21] (see also review articles [2,22–24]), there are very few works where the relaxation dynamics is studied for quadrupole nuclei in detail [25–27]. The dynamics of quadrupole nuclei is also discussed in Refs. [9,28,29].

In this paper we report on experimental study of spin dynamics of quadrupole nuclei in the singly charged (In,Ga)As/GaAs QDs. The nuclear spin polarization was studied in optical experiments by detection of the electron spin orientation via polarized secondary emission of the QDs in a transverse magnetic field (the Hanle effect). We have found that, when the photoluminescence (PL) of the samples under study is excited by light with the modulated helicity of polarization, the Hanle curves strongly depend on the modulation frequency. We have developed a phenomenological model based on the consideration of separate polarization dynamics of the $\pm 1/2$ nuclear spin doublets and of the split-off doublets, $\pm 3/2$, $\pm 5/2$, etc. The analysis performed using a pseudospin approach proposed in Ref. [30] has allowed us to extract contributions from polarization of these different groups of spin doublets into the effective nuclear field acting on the electron spin.

## II. EXPERIMENTAL DETAILS

We studied two samples prepared from one heterostructure with InAs/GaAs QDs grown by the Stranski-Krastanov method. Sample A was then annealed at temperature $T_{ann} = 900\,^{\circ}$C and sample B at temperature $T_{ann} = 980\,^{\circ}$C. The annealing gives rise to the diffusion of indium atoms into the barriers so that the indium concentration and, correspondingly, the crystal lattice deformations decrease at higher annealing temperatures. Theoretical modeling shows [31] that the deformation is of about 3% for sample A and 1% for sample B. The quadrupole splitting of the nuclear spin states strongly

 

depends on the deformation [32]. It is considerably smaller for sample B comparing to that for sample A. Therefore, the experimental study and analysis of two samples allows one to highlight the role of quadrupole splitting of nuclear states in the observed effects.

The QDs under study contain one resident electron per dot on average due to $\delta$-doping of barriers by donors during the epitaxial growth. There are 20 layers of the QDs with areal density of about $10^{10}$ cm$^{-2}$ separated by 60-nm-thick GaAs barriers [33]. Optical characterization of the samples is given in Ref. [34]. The photoluminescence (PL) band in sample A corresponding to the lowest optical transitions in the QDs is centered at photon energy $E_A = 1.34$ eV with the half width at half maximum (HWHM) $\delta E_A = 9$ meV. A similar PL band in sample B is shifted to the higher photon energy due to smaller indium content, $E_B = 1.42$ eV with $\delta E_B = 7$ meV.

In our present experiments, dependence of circular polarization of PL is measured as a function of the magnetic field applied perpendicular to the optical axis. The depolarization curves (Hanle curves) are measured under optical excitation by a continuous wave (cw) Ti:sapphire laser into the wetting layer of each sample ($E_{WL} = 1.459$ eV for sample A and $E_{WL} = 1.481$ eV for sample B). Polarization of the laser radiation is slowly modulated between $\sigma^+$ and $\sigma^-$ by an electro-optical modulator followed by a quarter-wave plate with a frequency varied from fractions of Hz to several kHz. No resonant effects studied in Refs. [34,35] are observed at such slow modulation of the polarization.

The PL is dispersed by a 0.5-m spectrometer and detected with a silicon avalanche photodiode. The circular polarization degree, $\rho = (I^{++} - I^{+-})/(I^{++} + I^{+-})$, is measured using a photoelastic modulator operating at a frequency of 50 kHz and a two-channel photon counting system. Here $I^{++}$ ($I^{+-}$) is the PL intensity for co- (cross-) circular polarization relative to that of excitation. In the maximum of the PL band of the QDs, the polarization is negative and reflects the mean spin polarization of resident electrons as was extensively discussed earlier [36,37]. Hereafter we use the maximal absolute value of $\rho$ obtained at the center of the PL band for each sample, $A_{NCP} = \max|\rho(\omega)|$, for the quantitative characteristic of the electron spin polarization [37], $S_z = A_{NCP}/2$, along the optical axis. Because the resident electrons are interacting with the QD nuclei, the negative circular polarization (NCP) can be used as a sensitive tool to monitor the nuclear spin state [37–39].

## III. EXPERIMENTAL RESULTS AND ANALYSIS

### A. Hanle curves at optical excitation with modulated polarization

Typical Hanle curves for different modulation periods of excitation polarization are shown in Fig. 1. As one can see, the Hanle curves for sample A [panel (a)] annealed at the lower temperature is considerably broader than the curves for sample B [panel (b)]. For both the samples, the shape of the Hanle curves strongly depends on the modulation period. At large periods as well as at the excitation with a fixed (cw) polarization, a well-resolved W structure is observed in small magnetic fields indicating a dynamic nuclear polarization (DNP) acting on electron spin as an effective nuclear field [40]. The W structure becomes smoothed and then almost disappears when the modulation period decreases. Besides, the Hanle curves noticeably shrink with the period shortening. At the smallest periods used in the experiments, the Hanle curves acquire almost Lorentzian shape. Experiments also show that the Hanle curve width monotonically decreases with the decrease of excitation power down to HWHM = 8 mT for sample A and HWHM = 1.5 mT for sample B at zero limit of excitation powers (not shown here). Such regularity is typical for depolarization of electron spins with no nuclear spin effects [1].

It is important that, in spite of the large overall modification of the Hanle curves, the polarization degree measured at zero magnetic fields is almost independent of modulation frequency. It approaches some value with the rise of excitation power and becomes also almost independent of the power at strong enough excitation. We assume that this stability of polarization indicates the total polarization of electron

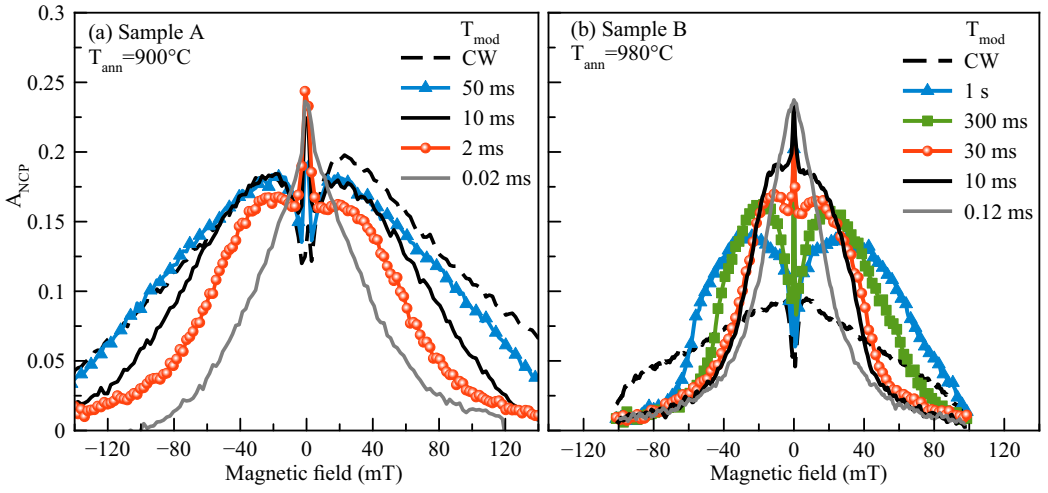


FIG. 1. Hanle curves for sample A (left panel) and sample B (right panel) measured at the optical excitation of one circular polarization (cw) as well as with the modulated polarization with periods given in the legends. Excitation power $P = 14$ mW for sample A and 10 mW for sample B. Diameter of laser spots on the samples, $d \approx 60$ $\mu$m. Sample temperature $T = 1.8$ K.

spins in the QDs at zero magnetic field. The deviation of the experimentally obtained value of the polarization from unity is most probably caused by contribution of nonpolarized PL from the neutral or doubly charged QDs [34].

Remarkable difference in behavior of the Hanle curves is observed for two samples studied; compare Fig. 1(a) and Fig. 1(b). Namely, for sample B with the higher annealing temperature, strong modification of the Hanle curve is observed even at large modulation period, $T_{\rm mod} = 1$ s, while for sample A the modification is hardly seen at the ten times shorter period. Besides, the Hanle curve narrowing for sample B is followed by a strong increase of polarization far beyond the W structure. No such increase is observed for sample A. This difference in the Hanle curve behavior indicates large difference in the dynamics of nuclear spin system in these two samples.

The analysis of the complex shape of the Hanle curves is the main topic of the rest of the paper. As shown in Ref. [21], the W structure and the shape of central part of the Hanle curves for the QDs under study can be well described in the framework of a phenomenological model. The model considers the electron spin precession about an effective magnetic field, which is the sum of the external magnetic field, $\mathbf{B}$, an effective field of the DNP (Overhauser field) [41], $\mathbf{B}_N$, and an effective field of the nuclear spin fluctuations, $\mathbf{B}_f$ [42].

In the GaAs-based structures with no quadrupole effects, the regular nuclear field is developed, in Hanle experiments, parallel rather than antiparallel to the external magnetic field because of the negative sign of the electron $g$ factor [1]. The W structure, in particular, the dips in the structure, are formed due to the large nuclear field, which magnifies the effect of small external magnetic field on the electron spin [21,40]. An increase of the magnetic field results in a decrease of the nuclear field and, correspondingly, in a partial recovery of the electron spin polarization that forms a W structure of the Hanle curve. At larger magnetic fields, i.e., at the wings of the Hanle curves, the electron polarization is effectively suppressed by the joint action of the external and nuclear magnetic field. Therefore, it would be expected that the modulation of excitation polarization suppressing the nuclear polarization should partially restore the electron polarization at the wings of the Hanle curve.

Experimentally observed evolution of the Hanle curves strongly differs from this prediction. As seen in Fig. 1, the increase of modulation frequency is followed by a smoothing of the W structure that indicates the decrease of nuclear polarization. At the same time, the width of the Hanle curves decreases, rather than increases, as predicted by the standard model [1].

We assume that the main reason for such behavior is the quadrupole effects in the nuclear spin system [7]. Due to presence of a gradient of crystal field, the spin doublets $\pm 3/2$, $\pm 5/2$, etc., are split-off from doublet $\pm 1/2$. In the structures under study, the gradient is mainly induced by the crystal lattice deformation. The principal axis of this deformation is directed along the growth axis of the structures that is along the optical axis in our experiments [32]. The quadrupole splitting caused by this deformation is studied in detail in Ref. [34].

At the presence of quadrupole splitting, behavior of the $\pm 1/2$ doublet and that of the split-off doublets in the magnetic field orthogonal to the deformation axis (the transverse field) are very different. Hereafter we call the components of nuclear field created by polarization of the $\pm 1/2$ and $\pm 3/2$, etc., doublets the dipole and quadrupole components, respectively. The dynamics of the dipole and quadrupole components is different because of strong suppression of the electron-nuclear flip-flop-mediated spin transitions between the $\pm 1/2$ and $\pm 3/2$, etc., states. The suppression comes from the large difference in the energy of the quadrupole splitting of nuclear spin states and of the Zeeman splitting of spin states of the resident electron so that the energy conservation rule cannot be satisfied in these transitions.

According to Ref. [7], the split-off nuclear spin states are weakly affected by the transverse magnetic field due to small effective nuclear $g$ factor and the quadrupole components of nuclear field conserve their orientation. Correspondingly, the electron spin polarization is also conserved due to hyperfine interaction with the stabilized nuclear spins. Only at large magnetic fields when the Zeeman splitting becomes comparable with the quadrupole splitting, the nuclear spins are no longer pinned to the major axis of the electric field gradient. Correspondingly, the nuclear spin orientation is destroyed and the electron polarization decreases that forms the wings of the Hanle curve.

The modulation of excitation polarization suppressing the quadrupole component of the nuclear field should result in narrowing the Hanle curve. The modulation-induced suppressing of the dipole component should modify the W structure of the Hanle curves. Different dependencies of the dipole and quadrupole components on the modulation frequency qualitatively explain complex behavior of the Hanle curves observed experimentally. An accurate analysis of the Hanle curves allowed us to obtain valuable information about dynamics of both the dipole and quadrupole components of the nuclear field.

### B. Phenomenological model

To extract information about the dynamics of nuclear polarization from the Hanle curves, we generalize the phenomenological model proposed in Ref. [21]. In particular, we consider two effective nuclear fields acting on the electron spin. The first one, the dipole field $\mathbf{B}_{Nd}$, is determined by polarization of the $\pm 1/2$ nuclear spin states. The second one, the quadrupole field $\mathbf{B}_{Nq}$, is due to the polarization of the split-off states $\pm 3/2$, etc. We should note that, in the (In,Ga)As-based structures, nuclei of all chemical elements, including isotopes constituting the structure, possess quadrupole moments.

The electron spin precesses in the total field, $\mathbf{B}_{\rm tot}$, consisting of several contributions:

$$\mathbf{B}_{\rm tot} = \mathbf{B} + \mathbf{B}_{Nd} + \mathbf{B}_{Nq} + \mathbf{B}_f, \tag{1}$$

where $\mathbf{B}_f$ is an effective field of the nuclear spin fluctuations. Due to the fast precession of electron spin about $\mathbf{B}_{\rm tot}$, only the projection, $S_{B_{\rm tot}}$, is conserved:

$$S_{B_{\rm tot}} = \frac{(\mathbf{S_0} \cdot \mathbf{B}_{\rm tot})}{|\mathbf{B}_{\rm tot}|} = S_0 \frac{B_{{\rm tot}z}}{\sqrt{B_{\rm tot}^2}}. \tag{2}$$

Here $S_0$ is the initial electron spin polarization created by optical excitation along the optical axis ($z$ axis). The

electron spin polarization measured in the experiments $S_z$ is the projection of $S_{B_{tot}}$ on the direction of observation (the optical axis). Correspondingly, the measured degree of PL polarization is

$$\rho = \frac{S_z}{S_0} = \frac{B_{\text{totz}}^2}{B_{\text{tot}}^2}. \tag{3}$$

The electron spin precession competes with the spin relaxation, which can be described by an effective field $B_\tau = \hbar/(g_e \mu_B \tau_{se})$ where $g_e$ is the electron $g$ factor, $\mu_B$ is the Bohr magneton, and $\tau_{se}$ is the electron spin relaxation time. To take into account the relaxation, we should generalize Eq. (3):

$$\rho = \frac{B_{\text{totz}}^2 + B_\tau^2}{B_{\text{tot}}^2 + B_\tau^2}. \tag{4}$$

For simplicity, we assume here that the relaxation time $\tau_{se}$ does not depend on the external magnetic field. This assumption will be verified by the simulations of Hanle curves described below. Similarly to Ref. [21], we assume that the total field squared can be expressed as

$$B_{\text{tot}}^2 = (B + B_{Ndx} + B_{Nqx})^2 + (B_{Ndz} + B_{Nqz})^2 + \langle B_f^2 \rangle. \tag{5}$$

Here we use the fact that the external magnetic field is directed along the $x$ axis. We also assume that no valuable nuclear polarization appears along the $y$ axis. The nuclear spin fluctuations are assumed to be isotropically distributed:

$$\langle B_f^2 \rangle = \langle B_{fx}^2 \rangle + \langle B_{fy}^2 \rangle + \langle B_{fz}^2 \rangle = 3 \langle B_{fz}^2 \rangle. \tag{6}$$

The $z$ projection of the total field squared, $B_{\text{totz}}^2$, is determined by a similar way with taking into account only $z$ components of the regular and fluctuating fields. Finally we obtain

$$\rho(B) = \frac{B_e}{B_e^0} = \frac{(B_{Ndz} + B_{Nqz})^2 + \langle B_{fz}^2 \rangle + B_\tau^2}{(B + B_{Ndx} + B_{Nqx})^2 + (B_{Ndz} + B_{Nqz})^2 + 3\langle B_{fz}^2 \rangle + B_\tau^2}. \tag{7}$$

Here $B_e = b_e S_z$ is the $z$ component of Knight field acting on the nuclei and $B_e^0 = b_e S_0$ is the Knight field at zero external magnetic field. Constant $b_e$ is proportional to the hyperfine interaction constant [1]. It is considered as a fitting parameter.

We suppose that components of the nuclear field, $B_{Nd\alpha}$ and $B_{Nq\alpha}$ with $\alpha = x,z$, are determined by the nuclear spin precession about the total field acting on the nuclei. The field consists of the external magnetic field, $B$, and of the Knight field, $B_e$. For simplicity, we neglect the $x$ and $y$ components of the Knight field because they are much smaller than the external magnetic field.

Evolution of the nuclear field created by nuclei with quadrupole splitting of spin states can be analyzed in the framework of a pseudospin model proposed in Ref. [30]. According to the model, each spin doublet with the spin projection, $m = \pm 1/2, \pm 3/2, \ldots$, onto the principal quadrupole axis may be considered independently, while the Zeeman splitting of the doublet in an external magnetic field is considerably smaller than the energy separation between the doublets determined by the quadrupole splitting. The Zeeman splitting, $\delta E_m = g_m \beta B$, can be described by an anisotropic nuclear $g$ factor, $g_m$. Here $\beta$ is the nuclear magneton. The nuclear spin polarization and, correspondingly, the nuclear field are created along an effective magnetic field, $\mathbf{B}_m^{eff} = g_{mx}\mathbf{B} + g_{mz}\mathbf{B}_e$ [43]. We should stress that the direction of $\mathbf{B}_m^{eff}$ deviates, in general case, from the direction of vector sum of fields $\mathbf{B}$ and $\mathbf{B}_e$ because of the anisotropy of the nuclear $g$ factor.

Using a simple vector model [21] one can obtain general expressions for components of nuclear field:

$$B_{N_{mz}} = B_{Nm} \frac{B_e^2}{(g_{mx}^* B)^2 + B_e^2},$$
$$B_{N_{mx}} = B_{Nm} \frac{(g_{mx}^* B) B_e}{(g_{mx}^* B)^2 + B_e^2}. \tag{8}$$

Here $B_{Nm} = B_{Nd}$ for $m = 1/2$ and $B_{Nm} = B_{Nq}$ for $m = 3/2$ are the dipole and quadrupole nuclear fields at zero external magnetic field. Their magnitude depends on the excitation power. We consider them as fitting parameters. In the case of In nuclei, there are also the nuclear spin doublets $m = 5/2, \ldots, 9/2$. Their contribution in the quadrupole nuclear field is found to be small as briefly discussed below (see Sec. III C). We neglect this contribution to minimize the number of fitting parameters.

Quantities $g_{mx}^* = g_{mx}/g_{mz}$ in Eqs. (8) are the normalized $g$ factors determined as the ratio of $g$ factors characterizing interactions with the magnetic fields applied across and along the principal quadrupole axis, respectively. In small transverse magnetic fields, the splitting of nuclear states with $m = \pm 1/2$ (the dipole states) linearly depends on the magnetic field and $g_{dx}^* \approx 2$, while the Zeeman splitting of the doublet is considerably smaller than the quadrupole splitting. We will use this approximate equality because, as will be seen in the next section, the dipole nuclear field significantly differs from zero only in small magnetic fields.

The splitting of the $\pm 3/2, \pm 5/2, \ldots$ doublets is strongly anisotropic in the transverse magnetic field and nonlinearly depends on the magnetic field magnitude. For nuclei with $I = 3/2$, splitting of the $\pm 3/2$ spin states is described by the expression [44]

$$\delta E_{\pm 3/2} = \frac{E_Q}{2}[a + (\sqrt{1 - a + a^2} - \sqrt{1 + a + a^2})], \tag{9}$$

where $a = 4\gamma\hbar B/E_Q$. Here $E_Q$ is the quadrupole splitting of the $\pm 1/2$ and $\pm 3/2$ doublets at zero magnetic field and $\gamma$ is the gyromagnetic ratio for the nuclei. Equation (9) allows one to obtain an exact expression for the nuclear $g$ factor. We found, however, that this complex expression can be well fitted for all the nuclei and magnetic fields considered here by

a phenomenological formula:

$$g^*_{qx} = k\frac{B^2}{B^2 + B^2_\Delta}, \tag{10}$$

where $k$ and $B_\Delta$ are the fitting parameters. According to this expression, the $g$ factor quadratically rises with magnetic field at small $B$ and then reaches a constant value at $B \gg B_\Delta$. An analysis shows that both the parameters are strongly different for Ga and As nuclei due to different quadrupole splittings. Therefore, to accurately model the nuclear field, a sum of contributions of different nuclei should be considered. The experimental results, however, do not contain sufficient information required for separation of the different contributions. We, therefore, simplify our analysis and suggest the simplest, linear, dependence for the $g$ factor,

$$g^*_{qx} = kB, \tag{11}$$

to model the effective quadrupole nuclear field averaged over all the nuclei. Results described in the next subsection show that this dependence allows us to explain the main peculiarities of the Hanle curves.

Substitution of expressions (8) into Eq. (7) gives rise to an equation of the 9th degree relative to Knight field $B_e$. Solution of this equation for different magnetic fields gives the field dependence of electron spin polarization that is the Hanle curve. Comparison of the modeled Hanle curve with that obtained experimentally allows us to determine fitting parameters $B_\tau$, $b_e$, $B_{Nd}$, $B_{Nq}$, $B_{fz}$, and $k$ for each modulation period.

To solve the problem we first obtained approximate values of the parameters. For this purpose we fixed one parameter, $b_e = 4$ mT for sample A and $b_e = 2$ mT for sample B, and obtained other parameters by simple fitting procedure using Eqs. (7) and (8). Then we solved the total equation using the obtained values of the parameters as the initial ones and setting the limits for their possible variations. We found that there is only one root of the equation, which satisfies the physical conditions: $S_z$ is the real and positive quantity.

Numerical solution of the equation for different magnetic fields allowed us to simulate Hanle curves by appropriate choice of the fitting parameters. We have ignored some asymmetry of Hanle curves observed experimentally (see Fig. 1) and simulated only a part of each Hanle curve measured at $B > 0$. An analysis has shown that the fitting parameters are not noticeably changed when another part of Hanle curves is modeled.

### C. Analysis of Hanle curves

The phenomenological model developed above allowed us to well describe the nontrivial shape of Hanle curves measured for both the samples at different modulation periods. Examples of the Hanle curves obtained in the model are shown in Fig. 2. Good correspondence of the measured and simulated Hanle curves allows us to obtain values of the fitting parameters at each modulation period and, therefore, to evaluate their frequency dependence. Although there are several fitting parameters, values of most the parameters can be determined independently because they control different features of Hanle curves. In particular, parameters $B_{Nd}$ and $B_{Nq}$, describing the photoinduced dipole and quadrupole nuclear spin polarization, determine the central part with W structure and the peripheral part of the Hanle curves, respectively.

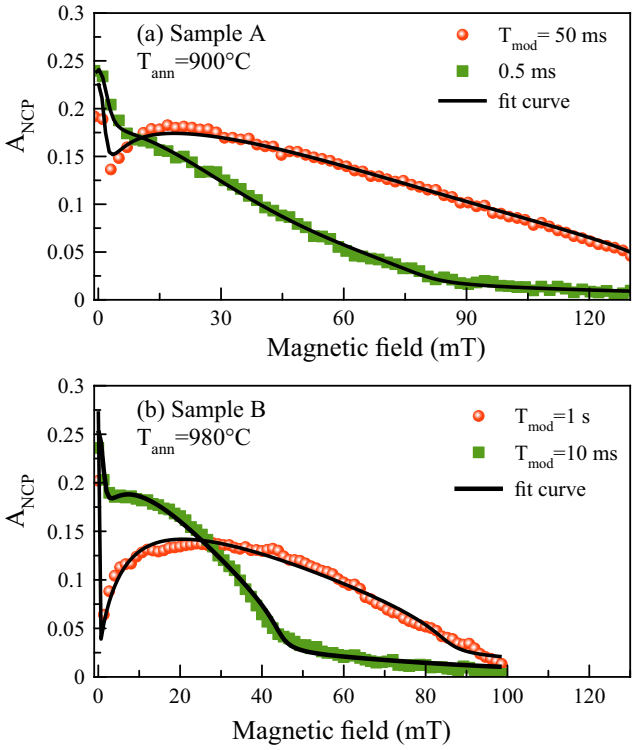


FIG. 2. Examples of the Hanle curve simulations for samples A (a) and B (b) for different modulation periods given in the legends. Symbols are the experimental data and solid lines are the fits.

Examples of magnetic field dependencies of the dipole and quadrupole components of nuclear field are shown in Fig. 3. As seen, the $x$ and $z$ components of the dipole field have large magnitude in small magnetic fields. In particular, the dipole component $B_{Ndz}$ has a maximal value at zero magnetic field and rapidly decreases with $B$ while component $B_{Ndx}$ rapidly rises in the same range of magnetic field (see inset in Fig. 3). As discussed in Ref. [21], such behavior of the nuclear field is responsible for the W structure in Hanle curves. Subsequent decrease of the $B_{Ndx}$ component with the further increase of external magnetic field completes the W structure. Beyond the W structure, i.e., in large magnetic fields, the dipole component of the nuclear field is virtually absent.

The quadrupole field is weakly changed in small magnetic fields. In particular, the $x$ component of the field is almost zero while the $z$ component has some finite, almost constant, value. It is the component which stabilizes the electron spin polarization making the Hanle curve broad at slow modulation of excitation polarization. At large external magnetic fields, the dipole field almost disappears and the wings of the Hanle curve are mainly determined by competition of the $x$ and $z$ components of the quadrupole field. As one can see in Fig. 3, the $z$ component rapidly decreases at large $B$ and the $x$ component increases that results in relatively sharp decrease of electron spin polarization observed experimentally. So, the dipole field forms the W structure and the quadrupole field forms the wings of the Hanle curve.

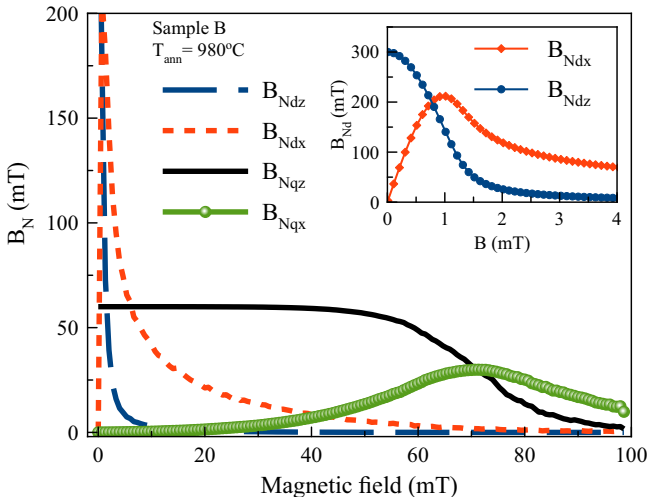


FIG. 3. Examples of the magnetic field dependencies of the longitudinal and transverse components of the dipole and quadrupole nuclear fields calculated for sample B using Eq. (8). The parameters used in the calculation are extracted from the Hanle curve measured at the modulation period $T_{\rm mod} = 300$ ms. The magnetic field dependence of $B_e$ is taken from the experimentally measured Hanle curve. Inset shows behavior of components of the dipole field at small magnetic fields. $B_{Ndz} = 300$ mT at zero magnetic field.

Let us now discuss other parameters of the model. Parameter $B_\tau$ is determined by time $\tau_{se}$ of the electron spin relaxation; see comment to Eq. (4). As mentioned above, $\tau_{se}$ and, correspondingly, $B_\tau$ depend on the excitation power but should be independent of the modulation period. Therefore we fixed the value $B_\tau = 18$ mT. This value is obtained from the Hanle curve width at the fastest modulation used when the nuclear spin effects are negligibly small.

Parameter $b_e$ [see Eq. (8)] characterizes the Knight field $B_e$ averaged over all the nuclei interacting with the electron spin. The magnitude of this parameter is determined by the electron density on the nuclei [1]. The described above simulations of the Hanle curves have shown that this parameter has to be changed under variation of the modulation period. In particular, $b_e = 5.3$ mT at slow modulation ($T_{\rm mod} > 0.01$ s) and $b_e = 8$ mT at fast modulation ($T_{\rm mod} < 0.01$ s) for sample A. For sample B, $b_e = 3.8$ mT at slow modulation ($T_{\rm mod} > 0.01$ s) and $b_e = 2.8$ mT at fast modulation ($T_{\rm mod} < 0.01$ s). We assume that this variation of $b_e$ with the modulation period is due to different rates of spin relaxation for different nuclear states. If the relaxation of some nuclear states is slower than the modulation period, such nuclear states are "switched off" from the joint electron-nuclear spin dynamics. Correspondingly, the Knight field should be averaged over a subset of nuclear states, which are not "switched off." Difference in the magnitudes of $b_e$ for samples A and B is explained by different electron densities on nuclei in these samples. Sample A contains QDs annealed at lower temperature ($T_{\rm ann} = 900\,^\circ$C) than the sample B ($T_{\rm ann} = 980\,^\circ$C) so that the indium content is larger, the electron localization volume is smaller, and the hyperfine interaction is stronger in sample A [31].

Parameter $k$ describing nonlinear splitting of the $\pm 3/2$ doublets in magnetic field [see Eq. (11)] is found to be almost independent of modulation period for both samples. Its average value is $k = 0.9 \times 10^{-4}$ mT$^{-1}$ for sample A and $k = 0.7 \times 10^{-4}$ mT$^{-1}$ for sample B. The obtained values of $k$ can be compared with those found from Zeeman splittings of the $\pm 3/2$ states in different nuclei. According to the data of Ref. [34], $k$(Ga) $= 20 \times 10^{-4}$ mT$^{-1}$, $k$(As) $= 1.3 \times 10^{-4}$ mT$^{-1}$ for sample A and $k$(Ga) $= 40 \times 10^{-4}$ mT$^{-1}$, $k$(As) $= 7 \times 10^{-4}$ mT$^{-1}$ for sample B. As seen, these values considerably differ for the Ga and As nuclei and are larger than those obtained from the modeling of Hanle curves.

A possible reason for this difference of $k$ obtained from the experimental data and from the splittings can be related to the fast phase relaxation of nuclear spin polarization caused by fluctuating electron spin polarization under strong optical pumping used in the experiments. An analysis shows [45] that this relaxation should additionally weaken the effect of transverse magnetic field on the nuclear spin dynamics.

Another possible reason is a contribution of the As nuclei in an asymmetric atomic configuration containing one or few In neighbors. The crystal field gradient caused by a statistical occupation of lattice nodes by the In and Ga atoms gives rise to a quadrupole splitting of spin states in the As nuclei [1]. The principal axis of the gradient may be oriented along different crystal axes. The quadrupole splitting in these nuclei is stronger; therefore the value of $k$ should be smaller. These nuclei can be responsible for stabilization of the electron spin polarization at large magnetic fields and, correspondingly, for the wings of Hanle curves observed experimentally. This contribution also explains the fact that the widths of the Hanle curves for sample A and sample B are not so strongly different (see Fig. 1) although the lattice deformation in sample A is three times larger compared to that in sample B [34].

Finally we should note that the contribution of In nuclei into the effect of stabilization of the electron spin polarization is negligible because of the wide spread of Zeeman splittings of different states ($m = \pm 3/2, \pm 5/2, \ldots, \pm 9/2$).

### D. Dynamics of nuclear fields

The simulation of Hanle curves described above allows us to analyze evolution of the dipole and quadrupole nuclear fields at the modulation of excitation polarization. Figure 4 shows the evolution of initial (photoinduced) values of nuclear fields $B_{Nd}$ and $B_{Nq}$ for both the samples. The magnitudes of nuclear fields, in particular, of the dipole component, obtained in the simulations have relatively large spread. As already discussed (see Fig. 3), the dipole component significantly differs from zero only at small magnetic fields in the range of the W structure of the Hanle curves. Therefore, any small inaccuracy of experimental data in this range noticeably affects the amplitude of this component obtained in the fitting. The quadrupole component is determined in the larger magnetic field range and, therefore, its magnitude is found with less uncertainty. Nevertheless, in spite of the spread, the obtained values of the dipole and quadrupole components demonstrate a certain tendency in evolution of the nuclear spin polarization.

As seen from Fig. 4, all the nuclear fields tend to go to some stationary values at slow enough modulation. These stationary values are very different for different nuclear fields and different samples. For sample A, as seen in Fig. 4(a), the

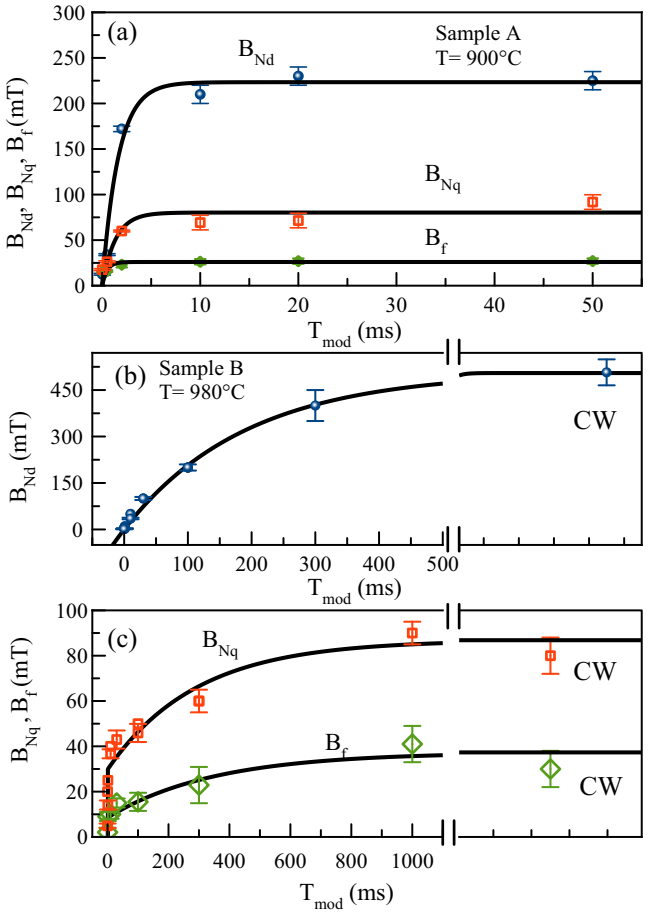


FIG. 4. Dependencies of the dipole field $B_{Nd}$, quadrupole field $B_{Nq}$, and the field of nuclear spin fluctuations $B_f$ on modulation period $T_{\rm mod}$ for sample A (a) and sample B [(b), (c)]. Symbols are the values extracted from the analysis of experimental data. Solid lines are the fits by Eqs. (12) and (13) with characteristic times as follows: for sample A, $\tau_{Nd} = 1.6 \pm 0.4$ ms, $\tau_{Nq} = 1.4 \pm 0.2$ ms, $\tau_f = 0.5 \pm 0.2$ ms; for sample B, $\tau_{Nd} = 190 \pm 11$ ms, $\tau_{1Nq} = 0.2 \pm 0.01$ ms, $\tau_{2Nq} = 330 \pm 80$ ms, $\tau_{1f} = 0.2 \pm 0.01$ ms, $\tau_{2f} = 470 \pm 80$ ms.

dipole field $B_{Nd}$ is only three times larger than the quadrupole field $B_{Nq}$. For the strongly annealed sample B, this difference is stronger; compare Figs. 4(b) and 4(c). As seen, the annealing noticeable increases the dipole field achievable at the cw or slowly modulated excitation.

Both the dipole and quadrupole fields decrease with shortening the modulation period. The decrease of nuclear fields is naturally explained by some inertia of the nuclear spin system, which does not allow it to be reoriented during the half-period of the modulation. This effect enables us to estimate the characteristic relaxation times for each nuclear field using a simple phenomenological function [46]:

$$B_N = B_{N\infty}\left[1 - \exp\left(-\frac{T_{\rm mod}}{\tau_N}\right)\right]. \tag{12}$$

This equation well describes evolution of the dipole and quadrupole nuclear fields in sample A and of the dipole field in sample B. At the same time, evolution of the quadrupole nuclear field in sample B cannot be fitted by this function and we have to use a more complicated fitting function:

$$B_N = B_{N\infty}\left[1 - a^2\exp\left(-\frac{T_{\rm mod}}{\tau_{N1}}\right) - b^2\exp\left(-\frac{T_{\rm mod}}{\tau_{N2}}\right)\right], \tag{13}$$

with condition $a^2 + b^2 = 1$. Here $B_{N\infty}$ is the value of nuclear field under the continuous wave excitation.

As follows from the fitting shown in Fig. 4, the relaxation time of the dipole field for the stronger annealed sample B is larger by about two orders of magnitude comparing to that for sample A. So drastic difference in the relaxation rates points out high sensitivity of the nuclear spin dynamics to quadrupole effects. We should mention also that the relaxation dynamics in bulk $n$-GaAs, where the quadrupole splitting is very small, is further slowed down by a few orders of magnitude [27,47–49].

Dynamics of quadrupole field in sample A is characterized by a relaxation time, which is close to that for the dipole field in this sample. In sample B, the dynamics of the quadrupole field is generally faster than that of the dipole field but consists of two components. The characteristic relaxation time of the fast component is close to that for sample A. The slow component is characterized by a large relaxation time of order that for the dipole component in this sample.

Fitting of the Hanle curves allowed us to obtain the effective field of nuclear spin fluctuations, $B_{fz}$. As one can see in Fig. 4, the amplitude of fluctuations decreases with decreasing period of the modulation. The dynamics of $B_{fz}$ is similar to dynamics of the quadrupole field and is characterized by a single relaxation time for sample A and two relaxation times for sample B.

## IV. DISCUSSION

The phenomenological model used above for analysis of experimental data is based on the approximation of the well-separated nuclear spin doublets. This approximation is valid in some limited range of the transverse magnetic field when the Zeeman splitting of the doublets is considerably smaller than the quadrupole splitting. However the experimental data analyzed in the present work are measured in the relatively wide range of magnetic field of about ±100 mT where the Zeeman and quadrupole splittings become comparable; see Ref. [34]. In such magnetic fields, the dipole $(\pm 1/2)$ and quadrupole $(\pm 3/2, \ldots)$ states are mixed that makes consideration of the dipole and quadrupole fields in large magnetic fields to be not applicable. A more accurate microscopic model is required for analysis of the spin dynamics in quadrupole nuclei. To the best of our knowledge, there is no such model so far. Therefore, we consider the results obtained in the framework of our model as a qualitative, rather than quantitative, characteristics of the nuclear spin system.

The most important experimental result is the drastic difference in evolution of the Hanle curves for two studied samples. As seen in Fig. 1 for sample A annealed at the lower temperature, the decrease of polarization modulation period of the excitation is followed by a decrease of the width of the Hanle curve with almost unchanged amplitude of its central part. Evolution of the Hanle curve for the strongly annealed

sample B is different. Namely, with the decrease of modulation period the amplitude of wings of the Hanle curve decreases while the amplitude of its central part beyond the W structure increases.

The analysis performed in the framework of the model described above allows us to conclude that the origin of such large difference in behavior of the Hanle curves for these samples is the large difference of relaxation rates of the dipole and quadrupole nuclear fields. This difference is particularly pronounced for the strongly annealed sample B where the dynamics of the quadrupole field is considerably faster than that of the dipole field; see Figs. 4(b) and 4(c). The slow modulation of excitation polarization suppresses first the long-lived dipole component of nuclear field in this sample. The component depolarizes electron spin because it is directed along the external magnetic field. Its suppression results in a recovery of the electron polarization. The quadrupole component of the nuclear field, whose relaxation is faster, is partially conserved at the slow modulation of polarization. It is directed along the optical axis and, therefore, stabilizes the electron spin polarization. Both effects of the slow modulation of excitation polarization make a contribution to the conservation of electron spin polarization responsible for the increase of the central part of the Hanle curve. The modulation at larger frequencies suppresses also the quadrupole nuclear field that results in a rapid depolarization of electron spin by the external magnetic field and hence in the narrowing of the Hanle curve. So the behavior of the Hanle curves observed in Fig. 1(b) is explained by the competition of the dipole and quadrupole components of nuclear fields.

In sample A, relaxation rates of the dipole and quadrupole components are similar [see Fig. 4(a)] and they are synchronously suppressed with the increase of modulation frequency. This is why the central part of the Hanle curves is weakly dependent on the modulation. Such dynamics in this sample is possibly caused by a mixing of the dipole and quadrupole nuclear spin states due to tilting of the principal axis of the electric field gradient tensor or presence of some biaxiality of the tensor observed for samples with low annealing temperature [32]. Similar although weaker distortions of the electric field gradient are, probably, responsible for the nonexponential dynamics of the quadrupole nuclear field in the strongly annealed sample B; see Fig. 4(c).

Although there are no doubts in the large difference in the relaxation rates of the dipole and quadrupole nuclear fields in sample B, the physical origin of this difference is unclear. One of the possible channels for fast relaxation of the quadrupole field is the relaxation $\pm 3/2 \rightarrow \pm 1/2$ caused by a modulation of the crystal field gradient. In particular, the crystal field gradient can be modulated by fluctuations of the carrier density [25–27]. In the case of QDs with a relatively deep potential well for carriers, the fluctuations are generally small, at least at low sample temperature. However, in the case of optical excitation of QDs, the fluctuations may be much larger due to separate capture of electrons and holes so that this mechanism of relaxation of the quadrupole states may become effective. After the $\pm 3/2 \rightarrow \pm 1/2$ relaxation, rapid precession of the nuclear spins in the transverse magnetic field mixes the $\pm 1/2$ states due to the large effective nuclear $g$ factor for this doublet. For example, the precession frequency is of order $10^4$ Hz in magnetic field of 1 mT. The backward relaxation $\pm 1/2 \rightarrow \pm 3/2$, which occurs at any moment of the precession, should give rise to effective destruction of the quadrupole field. This simplified picture of the relaxation process may explain the rapid relaxation of quadrupole field observed experimentally.

Finally we should mention one more effect observed at the modulation of excitation polarization. This is the suppression of the effective field of nuclear spin fluctuations, which is observed at the shortening of the modulation period [Fig. 4(c)]. The suppression unambiguously follows from the fact of the strong narrowing of the Hanle curve down to the purely electron peak at the fast enough modulation of polarization. We assume that the strong optical pumping with rapidly alternating polarization may equalize the population of nuclear states with spin down and spin up and, hence, partially suppress the nuclear spin fluctuations, which supports orientation of the electron spin [50]. The mentioned above almost total coincidence of the dynamics of the nuclear spin fluctuation and of the quadrupole nuclear field suggests that the quadrupole states mainly contribute to the nuclear spin fluctuations. A similar conclusion has been made in Ref. [51]. Theoretical analysis of such behavior of the nuclear spin fluctuations for the quadrupole nuclei requires a quantum-mechanical modeling with a huge number of spin degrees of freedom, which is out of the scope of the present work.

## V. CONCLUSION

Strong modification of Hanle curves observed under modulation of excitation polarization is demonstrated to contain valuable information about the dynamics of coupled electron-nuclear spin systems in the studied (In,Ga)As/GaAs QDs. To extract this information, we have developed a simplified phenomenological model considering separate dynamics of the dipole and quadrupole nuclear fields. In particular, the quadrupole field can efficiently stabilize electron spin polarization in large magnetic fields up to 100 mT. At the same time, the relatively fast relaxation of polarization of the quadrupole nuclear states may considerably shorten the electron spin lifetime. In the studied samples with different quadrupole splittings, the lifetimes differ by about two orders of magnitude.

## ACKNOWLEDGMENTS

The authors thank K. V. Kavokin for fruitful discussion. The work is supported by the Russian Foundation for Basic Research (Project No. 15-52-12020) and the Deutsche Forschungsgemeinschaft in the frame of International Collaborative Research Center TRR160. I.V.I. acknowledges the support of the Russian Foundation for Basic Research (Contract No. 16-02-00245A) and SPbU (Grant No. 11.38.213.2014).

[1] V. G. Fleisher and I. A. Merkulov, in *Optical Orientation*, edited by B. P. Zakharchenya and F. Meier (North-Holland, Amsterdam, 1984), Chap. 5.

[2] V. K. Kalevich, K. V. Kavokin, and I. A. Merkulov, in *Spin Physics in Semiconductors*, edited by M. I. Dyakonov (Springer-Verlag, Berlin, 2008), Chap. 11.

[3] B. E. Kan, A silicon-based nuclear spin quantum computer, Nature (London) **393**, 133 (1998).

[4] J. M. Taylor, C. M. Marcus, and M. D. Lukin, Long-Lived Memory for Mesoscopic Quantum Bits, Phys. Rev. Lett. **90**, 206803 (2003).

[5] C. Boehme and D. R. McCamey, Nuclear-spin quantum memory poised to take the lead, Science **336**, 1239 (2012).

[6] R. Oulton, A. Greilich, S. Yu. Verbin, R. V. Cherbunin, T. Auer, D. R. Yakovlev, M. Bayer, I. A. Merkulov, V. Stavarache, D. Reuter, and A. D. Wieck, Subsecond Spin Relaxation Times in Quantum Dots at Zero Applied Magnetic Field Due to a Strong Electron-Nuclear Interaction, Phys. Rev. Lett. **98**, 107401 (2007).

[7] R. I. Dzhioev and V. L. Korenev, Stabilization of the Electron-Nuclear Spin Orientation in Quantum Dots by the Nuclear Quadrupole Interaction, Phys. Rev. Lett. **99**, 037401 (2007).

[8] D. Gammon, Al. L. Efros, T. A. Kennedy, M. Rosen, D. S. Katzer, D. Park, S. W. Brown, V. L. Korenev, and I. A. Merkulov, Electron and Nuclear Spin Interactions in the Optical Spectra of Single GaAs Quantum Dots, Phys. Rev. Lett. **86**, 5176 (2001).

[9] P. Maletinsky, A. Badolato, and A. Imamoglu, Dynamics of Quantum Dot Nuclear Spin Polarization Controlled by a Single Electron, Phys. Rev. Lett. **99**, 056804 (2007).

[10] I. A. Akimov, D. H. Feng, and F. Henneberger, Electron Spin Dynamics in a Self-Assembled Semiconductor Quantum Dot: The Limit of Low Magnetic Fields, Phys. Rev. Lett. **97**, 056602 (2006).

[11] B. Eble, O. Krebs, A. Lemíatre, K. Kowalik, A. Kudelski, P. Voisin, B. Urbaszek, X. Marie, and T. Amand, Dynamic nuclear polarization of a single charge-tunable InAs/GaAs quantum dot, Phys. Rev. B **74**, 081306(R) (2006).

[12] A. I. Tartakovskii, T. Wright, A. Russell, V. I. Fal'ko, A. B. Van'kov, J. Skiba-Szymanska, I. Drouzas, R. S. Kolodka, M S. Skolnick, P. W. Fry, A. Tahraoui, H.-Y. Liu, and M. Hopkinson, Nuclear Spin Switch in Semiconductor Quantum Dots, Phys. Rev. Lett. **98**, 026806 (2007).

[13] T. Belhadj, T. Kuroda, C.-M. Simon, T. Amand, T. Mano, K. Sakoda, N. I. Koguchi, X. Marie, and B. Urbaszek, Optically monitored nuclear spin dynamics in individual GaAs quantum dots grown by droplet epitaxy, Phys. Rev. B **78**, 205325 (2008).

[14] J. Skiba-Szymanska, E. A. Chekhovich, A. E. Nikolaenko, A. I. Tartakovskii, M. N. Makhonin, I. Drouzas, M. S. Skolnick, and A. B. Krysa, Overhauser effect in individual InP/$Ga_xIn_{1-x}$P dots, Phys. Rev. B **77**, 165338 (2008).

[15] O. Krebs, P. Maletinsky, T. Amand, B. Urbaszek, A. Lemaître, P. Voisin, X. Marie, and A. Imamoglu, Anomalous Hanle Effect due to Optically Created Transverse Overhauser Field in Single InAs/GaAs Quantum Dots, Phys. Rev. Lett. **104**, 056603 (2010).

[16] E. A. Chekhovich, M. N. Makhonin, K. V. Kavokin, A. B. Krysa, M. S. Skolnick, and A. I. Tartakovskii, Pumping of Nuclear Spins by Optical Excitation of Spin-Forbidden Transitions in a Quantum Dot, Phys. Rev. Lett. **104**, 066804 (2010).

[17] E. A. Chekhovich, K. V. Kavokin, J. Puebla, A. B. Krysa, M. Hopkinson, A. D. Andreev, A M. Sanchez, R. Beanland, M. S. Skolnick, and A. I. Tartakovskii, Structural analysis of strained quantum dots using nuclear magnetic resonance, Nat. Nanotechnol. **7**, 646 (2012).

[18] A. Högele, M. Kroner, C. Latta, M. Claassen, I. Carusotto, C. Bulutay, and A. Imamoglu, Dynamic Nuclear Spin Polarization in the Resonant Laser Excitation of an InGaAs Quantum Dot, Phys. Rev. Lett. **108**, 197403 (2012).

[19] R. V. Cherbunin, S. Yu. Verbin, T. Auer, D. R. Yakovlev, D. Reuter, A. D. Wieck, I. Ya. Gerlovin, I. V. Ignatiev, D. V. Vishnevsky, and M. Bayer, Dynamics of the nuclear spin polarization by optically oriented electrons in a (In, Ga)As/GaAs quantum dot ensemble, Phys. Rev. B **80**, 035326 (2009).

[20] S. Yu. Verbin, I. Ya. Gerlovin, I. V. Ignatiev, M. S. Kuznetsova, R. V. Cherbunin, K. Flisinski, D. R. Yakovlev, and M. Bayer, Dynamics of nuclear polarization in InGaAs quantum dots in a transverse magnetic field, J. Exp. Theor. Phys. **114**, 681 (2012).

[21] M. S. Kuznetsova, K. Flisinski, I. Ya. Gerlovin, I. V. Ignatiev, K. V. Kavokin, S. Yu. Verbin, D. Reuter, A. D. Wieck, D. R. Yakovlev, and M. Bayer, Hanle effect in (In, Ga)As quantum dots: Role of nuclear spin fluctuations, Phys. Rev. B **87**, 235320 (2013).

[22] W. A. Coish and J. Baugh, Nuclear spins in nanostructures, Phys. Status Solidi B **246**, 2203 (2009).

[23] E. A. Chekhovich, M. N. Makhonin, A. I. Tartakovskii, A. Yacoby, H. Bluhm, K. C. Nowack, and L. M. K. Vandersypen, Nuclear spin effects in semiconductor quantum dots, Nat. Mater. **12**, 494 (2013).

[24] B. Urbaszek, X. Marie, T. Amand, O. Krebs, P. Voisin, P. Malentinsky, A. Högele, and A. Imamoglu, Nuclear spin physics in quantum dots: An optical investigation, Rev. Mod. Phys. **85**, 79 (2013).

[25] C. Deng and X. Hu, Selective dynamic nuclear spin polarization in a spin-blocked double dot, Phys. Rev. B **71**, 033307 (2005).

[26] D. Paget, T. Amand, and J.-P. Korb, Light-induced nuclear quadrupolar relaxation in semiconductors, Phys. Rev. B **77**, 245201 (2008).

[27] M. Kotur, R. I. Dzhioev, M. Vladimirova, B. Jouault, V. L. Korenev, and K. V. Kavokin, Nuclear spin warm up in bulk *n*-GaAs, Phys. Rev. B **94**, 081201 (2016).

[28] E. A. Chekhovich, M. N. Makhonin, J. Skiba-Szymanska, A. B. Krysa, V. D. Kulakovskii, M. S. Skolnick, and A. I. Tartakovskii, Dynamics of optically induced nuclear spin polarization in individual InP/$Ga_xIn_{1-x}$P quantum dots, Phys. Rev. B **81**, 245308 (2010).

[29] C. Latta, A. Srivastava, and A. C. Imamoglu, Hyperfine Interaction-Dominated Dynamics of Nuclear Spins in Self-Assembled InGaAs Quantum Dots, Phys. Rev. Lett. **107**, 167401 (2011).

[30] E. S. Artemova and I. A. Merkulov, Theory of nuclear polarization in semiconductors by polarized electrons in the presence of strong quadrupole splitting of nuclear spin levels, Fiz. Tv. Tela **27**, 1150 (1985) [Sov. Phys. Solid State **27**, 694 (1985)].

[31] M. Yu. Petrov, I. V. Ignatiev, S. V. Poltavtsev, A. Greilich, A. Bauschulte, D. R. Yakovlev, and M. Bayer, Effect of thermal annealing on the hyperfine interaction in InAs/GaAs quantum dots, Phys. Rev. B **78**, 045315 (2008).

[32] P. S. Sokolov, M. Yu. Petrov, T. Mehrtens, K. Müller-Caspary, A. Rosenauer, D. Reuter, and A. D. Wieck, Reconstruction of nuclear quadrupole interaction in (In, Ga)As/GaAs quantum

dots observed by transmission electron microscopy, Phys. Rev. B **93**, 045301 (2016).

[33] A. Greilich, R. Oulton, E. A. Zhukov, I. A. Yugova, D. R. Yakovlev, M. Bayer, A. Shabaev, Al. L. Efros, I. A. Merkulov, V. Stavarache, D. Reuter, and A. Wieck, Optical Control of Spin Coherence in Singly Charged (In, Ga)As/GaAs Quantum Dots, Phys. Rev. Lett. **96**, 227401 (2006).

[34] M. S. Kuznetsova, K. Flisinski, I. Ya. Gerlovin, M. Yu. Petrov, I. V. Ignatiev, S. Yu. Verbin, D. R. Yakovlev, D. Reuter, A. D. Wieck, and M. Bayer, Nuclear magnetic resonances in (In, Ga)As/GaAs quantum dots studied by resonant optical pumping, Phys. Rev. B **89**, 125304 (2014).

[35] K. Flisinski, I. Ya. Gerlovin, I. V. Ignatiev, M. Yu. Petrov, S. Yu. Verbin, D. R. Yakovlev, D. Reuter, A. D. Wieck, and M. Bayer, Optically detected magnetic resonance at the quadrupole-split nuclear states in (In, Ga)As/GaAs quantum dots, Phys. Rev. B **82**, 081308(R) (2010).

[36] R. V. Cherbunin, K. Flisinski, I. Ya. Gerlovin, I. V. Ignatiev, M. S. Kuznetsova, M. Yu. Petrov, D. R. Yakovlev, D. Reuter, A. D. Wieck, and M. Bayer, Resonant nuclear spin pumping in (In, Ga)As quantum dots, Phys. Rev. B **84**, 041304 (2011).

[37] I. V. Ignatiev, S. Yu. Verbin, I. Ya. Gerlovin, R. V. Cherbunin, and Y. Masumoto, Negative circular polarization of InP QD luminescence: Mechanism of formation and main regularities, Optica i Spektroskopiya. **106**, 427 (2009) [Opt. Spektr. **106**, 375 (2009)].

[38] S. Cortez, O. Krebs, S. Laurent, M. Senes, X. Marie, P. Voisin, R. Ferreira, G. Bastard, J.-M. Gérard, and T. Amand, Optically Driven Spin Memory in *n*-Doped InAs-GaAs Quantum Dots, Phys. Rev. Lett. **89**, 207401 (2002).

[39] A. Shabaev, E. A. Stinaff, A. S. Bracker, D. Gammon, A. L. Efros, V. L. Korenev, and I. Merkulov, Optical pumping and negative luminescence polarization in charged GaAs quantum dots, Phys. Rev. B **79**, 035322 (2009).

[40] D. Paget, G. Lampel, B. Sapoval, and V. I. Safarov, Low field electron-nuclear spin coupling in gallium arsenide under optical pumping conditions, Phys. Rev. B **15**, 5780 (1977).

[41] A. W. Overhauser, Polarization of nuclei in metals, Phys. Rev. **92**, 411 (1953).

[42] I. A. Merkulov, Al. L. Efros, and M. Rosen, Electron spin relaxation by nuclei in semiconductor quantum dots, Phys. Rev. B **65**, 205309 (2002).

[43] Here we take into account that the electron $g$ factor is isotropic so that the electron "feels" the effective nuclear field, which direction coincides with that of nuclear spin polarization.

[44] A. Abragam, *Principles of Nuclear Magnetism* (Oxford University Press, London 1962).

[45] K. V. Kavokin (private communication).

[46] A theoretical analysis of the nuclear spin relaxation performed in a paper by F. Heisterkamp, E. A. Zhukov, A. Greilich, D. R. Yakovlev, V. L. Korenev, A. Pawlis, and M. Bayer [Phys. Rev. B **91**, 235432 (2015)] gives rise to another time dependence, which, however, is well modeled by Eq. (12) with close values of effective time constants.

[47] V. K. Kalevich, V. D. Kulkov, and V. G. Fleisher, Onset of a nuclear polarization front due to optical spin orientation in a semiconductor, Pis'ma Zh. Eksp. Teor. Fiz. **35**, 17 (1982) [JETP Lett. **35**, 20 (1982)].

[48] I. I. Ryzhov, S. V. Poltavtsev, K. V. Kavokin, M. M. Glazov, G. G. Kozlov, M. Vladimirova, D. Scalbert, S. Cronenberger, A. V. Kavokin, A. Lemaítre, J. Bloch, and V. S. Zapasskii, Measurements of nuclear spin dynamics by spin-noise spectroscopy, Appl. Phys. Lett. **106**, 242405 (2015).

[49] I. I. Ryzhov, G. G. Kozlov, D. S. Smirnov, M. M. Glazov, Y. P. Efimov, S. A. Eliseev, V. A. Lovtcius, V. V. Petrov, K. V. Kavokin, A. V. Kavokin, and V. S. Zapasski, Spin noise explores local magnetic fields in a semiconductor, Sci. Rep. **6**, 21062 (2016).

[50] G. Wüst, M. Munsch, F. Maier, An. V. Kuhlmann, A. Ludwig, A. D. Wieck, D. Loss, M. Poggio, and R. J. Warburton, Role of the electron spin in determining the coherence of the nuclear spins in a quantum dot, Nat. Nanotechnol. **11**, 885 (2016).

[51] N. A. Sinitsyn, Yan Li, S. A. Crooker, A. Saxena, and D. L. Smith, Role of Nuclear Quadrupole Coupling on Decoherence and Relaxation of Central Spins in Quantum Dots, Phys. Rev. Lett. **109**, 166605 (2012).